

CFD Analysis of Single Flow Solar Air Heater with Double ARC Roughness

Jitendra Kumar Mishra¹, A.P. Vijaykant Pandey²

¹PG Student, RKDF College of Technology, Bhopal, India

²PG Guide and Assistant Professor, RKDF College of Technology, Bhopal, India

Abstract: Artificial roughness is used for enhancement of thermal performance of solar air heaters in the form of repeated ribs has been proposed as a convenient method. This thesis presents the CFD investigation of heat transfer and friction factor characteristics of a rectangular duct roughened with repeated Double arc, on one broad wall arranged at an inclination with respect to the flow direction. The duct has a width to height ratio (W/H) of 8, relative roughness pitch (P/e) of 10, relative roughness height (e/Dh) of 0.044, and arc angle of 15°, 30° & 45°. The comparison of heat transfer and friction characteristics of roughened duct and smooth duct under similar flow condition is simulated in this. The effect of change in angle of attack in flow having Reynolds numbers from 2000 to 16,000. The maximum enhancement in Nusselt number and friction factor is observed to be 1.69 and 1.79 times of that of the smooth duct, respectively. The thermo-hydraulic performance parameter is found to be the maximum for the arc angle of 30°.

Keywords: Rectangular Duct, Double Arc, Nusselt No., Friction Factor

1. Introduction

Due to a growing world population and increasing modernization, global energy demand is projected to more than double during the first half of the twenty-first century and to more than triple by the end of the century. Presently, the world's population is nearly 7 billion, and projections are for a global population approaching 10 billion by midcentury. Future energy demands can only be met by introducing an increasing percentage of alternative fuels. Incremental improvements in existing energy networks will be inadequate to meet this growing energy demand. Due to dwindling reserves and ever-growing concerns over the impact of burning carbon fuels on global climate change, fossil fuel sources cannot be exploited as in the past.

Finding sufficient supplies of clean and sustainable energy for the future is the global society's most daunting challenge for the twenty-first century. The future will be a mix of energy technologies with renewable sources such as solar, wind, and biomass playing an increasingly important role in the new global energy economy. The key question is: How long it will take for this sustainable energy changeover to occur? And how much environmental, political, and economic damage is acceptable in the meantime? If the twenty-first century sustainable energy challenge is not met quickly, many less-developed countries will suffer major famines and social instability from rising energy prices. Ultimately, the world's economic order is at stake.

Approximately one-third of the world's population lives in rural regions without access to the electric grid, and about half of these same people live without access to safe and clean water. Solar energy is unique in that it can easily provide electricity and purified water for these people today with minimal infrastructure requirements by using local energy resources that promote local economic development.

2. Literature Review

The use of artificial roughness in the form of repeated ribs has been found to be an efficient method of enhancing the heat transfer to fluid flowing in the duct. Detailed information about the heat transfer and flow characteristics in ribbed ducts is very important in designing Solar air Heater Ducts, Heat Exchangers and cooling systems of gas turbine engines. The application of artificial roughness in the form of fine wires and ribs of different shapes has been recommended to enhance the heat transfer coefficient by several investigators. It has been found that the main thermal resistance to the convective heat transfer is due to the presence of laminar sub layer on the heat-transferring surface. The ribs break the laminar sub layer and create local wall turbulence due to flow separation and reattachment between consecutive ribs, which reduce the thermal resistance and greatly enhance the heat transfer. However, the use of artificial roughness results in higher friction and hence higher pumping power requirements. Therefore, it is desirable that the turbulence should be created in the vicinity of the wall, i.e. only in the laminar sub-layer region, which is responsible for thermal resistance. Hence, the efforts of researchers have been directed towards finding the roughness shape and arrangement, which break the laminar sub-layer, enhance the heat transfer coefficient most with minimum pumping power penalty.

Lanjewar et al.[1] Concept of artificial roughness on plain surface is an important technique to enhance heat transfer rate of air flowing in solar air heater. Over the years different rib geometries have been designed to investigate heat transfer and friction characteristics of solar air heater. In this paper an attempt is made to review development of different rib geometries employed for creating artificial roughness. Heat transfer and friction factor correlations developed by various investigators are presented. Performance evaluation for different orientations of double arc rib roughness is presented.

Gabhane et al. [2] The Thermal and hydraulic performance of Double Flow Solar Air Heater (SAH) roughened with multiple C-shape rib was investigated experimentally. Three rib angles were used for different rib geometries with varying pitch distance, an angle of attack and Reynolds number. Multiple C-shaped ribs in double flow arrangement provides better heat transfer than other arrangements. Correlations were developed for Nusselt number, friction factor, Stanton number and Thermo hydraulic performance parameter to increase the usefulness of result.

Pandey et al.[3] In this present article an experimental study has been carried out on heat transfer and friction factor in rectangular channel which is having multiple-arc shaped with gaps as roughness element. The investigation encompassed Reynolds number (Re) ranges from 2100 to 21,000 (7 values), relative roughness height (e/D) ranges from 0.016 to 0.044 (4 values), relative roughness pitch (p/e) ranges from 4 to 16 (4 values), arc angle (a) values are 30–75_ (4 values), relative roughness width (W/w) ranges from 1 to 7 (5 values), relative gap distance (d/x) values are 0.25–0.85 (4 values) and relative gap width (g/e) ranges from 0.5 to 2.0 (4 values). The maximum increment in Nusselt number (Nu) and friction factor (f) is 5.85 and 4.96 times in comparison to the smooth duct. Utilizing these data, correlations were developed for Nu and f.

Aharwal et al.[4] Artificial roughness in the form of repeated ribs has been proposed as a convenient method for enhancement of thermal performance of solar air heaters. This paper presents the experimental investigation of heat transfer and friction factor characteristics of a rectangular duct roughened with repeated square cross-section split-rib with a gap, on one broad wall arranged at an inclination with respect to the flow direction. The duct has a width to height ratio (W/H) of 5.84, relative roughness pitch (P/e) of 10, relative roughness height λ (e/Dh) of 0.0377, and angle of attack (a) of 60.1. The gap width (g/e) and gap position (d/W) were varied in the range of 0.5–2 and 0.1667–0.667, respectively. The heat transfer and friction characteristics of this roughened duct have been compared with those of the smooth duct under similar flow condition. The effect of gap position and gap width has been investigated for the range of flow Reynolds numbers from 3000 to 18,000. The maximum enhancement in Nusselt number and friction factor is observed to be 2.59 and 2.87 times of that of the smooth duct, respectively. The thermo-hydraulic performance parameter is found to be the maximum for the relative gap width of 1.0 and the relative gap position of 0.25.

Han et al. [4] experimentally investigated the effects of rib shape, angle of attack and pitch-to-rib height ratio on friction factor and heat transfer coefficient. Author reported that ribs with 45° inclinations produced better heat transfer performance than ribs with 90° orientations, when compared at the same friction power.

Han [5] investigated the developing heat transfer in rectangular channels with rib turbulators for rib angle varying from 90° to 30°. The combined effects of rib angle and channel aspect ratio on local heat transfer coefficient were studied. The results indicate that the best heat transfer in square channel was obtained with angled ribs at 30- 45°

and was about 30% higher than the 90° transverse ribs for constant pumping power. However, for rectangular channel with aspect ratio of 2 and 4, the heat transfer enhancement using 30°-45° ribs was only 5% more than the 90° transverse rib. In general, it was noted that in square channel the heat transfer increased with decrease in rib angle whereas in rectangular channel the dependence of heat transfer on rib angle was negligible.

Verma and Prasad [6] developed the relations to calculate the average friction factor and Stanton number for artificial roughness of absorber plate by small diameter protrusion wire. They used these relations to compare the effect of height and pitch of roughness element on heat transfer and friction factor with already available experimental data. The friction factor for one side rough duct is determined by assuming that the total shear force in the one side rough duct is approximately equal to the combined shear force from three smooth walls in a four-sided smooth duct and the shear force from one rough wall in a four-sided rough duct. They used the friction similarity law and heat–momentum transfer analogy

Han et al. [7] studied a square channel with two ribbed walls for five different rib profiles. Their study illustrated that rib tabulators with greater number of sharp corners yield increasingly higher heat transfer coefficient as well as pressure drop.

Chandra et al. [8] carried out an experimental study of surface heat transfer and friction characteristics of a fully developed turbulent air flow in a square channel with transverse ribs on one, two, three, and four walls. Tests were performed for Reynolds numbers ranging from 10,000 to 80,000. The pitch to rib height ratio, P/e, was kept at 8 and rib height to channel hydraulic diameter ratio, e/D was kept at 0.0625. The channel length to hydraulic diameter ratio, L/D, was 20. The heat transfer coefficient and friction factor results were enhanced with the increase in the number of ribbed walls. The friction roughness function, $R(e^+)$, was almost constant over the entire range of tests performed and was within comparable limits of the previously published data. The heat transfer roughness function, $G(e^+)$, increased with roughness Reynolds number and compared well with previous work in this area. Both correlations could be used to predict the friction factor and heat transfer coefficient in a rectangular channel with varying number of ribbed walls. The results of could be used in various applications of turbulent internal channel flows involving different number of rib roughened walls.

Gupta et al. [9] carried out an experimental investigation on solar air heater with angled ribs with circular cross-section. They have investigated the effect of relative roughness height (e/D), inclination of rib with respect to flow direction and Reynolds number on fluid flow characteristics in transitionally rough flow region and evaluated the thermo hydraulic performance of solar air heaters.

Zhang et al. [10] observed that deploying of groove in between the ribs enhances the turbulences as well as reattaches the free shear layer nearer to the rib. They have reported that the addition of grooves in between adjacent

square ribs enhances the heat transfer capability of the surface considerably with nearly same pressure drop penalty. It appears that it will be fruitful to investigate an artificially roughened surface with optimally chamfered rib combined with grooves present between two ribs in order to achieve further decrease in relative roughness pitch and enhancement of heat transfer rate from such a surface. In view of the above an experimental investigation has been planned to investigate the heat and fluid flow characteristics of artificially roughened surface with chamfered rib-grooved roughness.

Park et al. [11] presented the results of heat transfer and friction factor data measured in five short rectangular channels with turbulence promoters. Author investigated the combined effects of the channel aspect ratio, rib angle of attack, and flow Reynolds number on heat transfer and pressure drop in rectangular channels with two opposite ribbed walls. The channel aspect ratio (width to height, W/H , ribs on side W) varied from $1/4$ to $1/2$, to 1, 2 and 4, while the corresponding rib angles of attack were 90° , 60° , 45° , and 30° , respectively. The Reynolds number range was 10,000–60,000. The results suggested that the narrow aspect ratio channels ($W/H < 1$) gave much better heat transfer performance than the wide aspect ratio channels ($W/H > 1$). For the square channel ($W/H = 1$), the $60^\circ/45^\circ$ angled ribs provided the best heat transfer performance. For the narrow aspect ratio channel ($W/H=1/4$ or $1/2$), the $45^\circ/60^\circ$ angled ribs were recommended while the $30^\circ/45^\circ$ angled ribs were better for wide aspect ratio channels ($W/H = 4$ or 2).

Computational fluid dynamics

In computer-based simulation the Computational fluid dynamics or CFD is the system of analysis involving fluid flow, heat transfer and associated phenomena such as chemical reactions. This technique is very powerful for industrial and non-industrial application areas and spans a wide range for this. Some examples are:

- Lift and drag in aerodynamics of aircraft and vehicles
- Hydrodynamics of ships
- Power plant: combustion in internal combustion engines and gas turbines
- Flows inside rotating passages, diffusers etc. in turbo machinery.
- Cooling of equipment including microcircuits in electrical and electronic engineering.
- Mixing and separation, polymer moulding in chemical process engineering.
- Wind loading and heating/ventilation in external and internal environment of buildings.
- Marine engineering: loads on off-shore structures
- Environmental engineering: distribution of pollutants and effluents
- Hydrology and oceanography: flows in rivers, estuaries, oceans
- Meteorology: weather prediction
- Biomedical engineering: blood flows through arteries and veins

The equations governing the fluid flow are the continuity (conservation of mass), the Navier-Stokes (balance of momentum), and the energy (conservation of energy) equations. These equations form a system of coupled non-linear partial differential equations (PDEs). Because of the couple nature of equation and the presence of non-linear term, the fluid-flow equation is generally not applicable to analytical method for obtain the solution. In general, closed form analytical solutions are possible only if these PDEs can be made linear, either because non-linear terms naturally drop out (as in the case of parallel flows or flows that are inviscid and irrotational everywhere) or because the nonlinear terms are small compared to other terms so that they can be neglected (e.g., creeping flows, small amplitude sloshing of liquid etc.). If the non-linearities in the governing PDEs cannot be neglected, which is often the case for most engineering flows, one normally has to resort to numerical methods to obtain solutions.

CFD is used to re-placed the governing equation of Flow of fluid, with a set of algebraic equation (this process is called discretization), which in turn can be solved to get an approximate solution with the aid of a digital-computer. The commonly used discretization methods in CFD analysis are the finite difference method (FDM), the finite volume method (FVM), the finite element method (FEM), and the boundary element method (BEM). Some special cases of flow problems can also be solved using nonstandard method like, boundary integral methods, spectral methods, and pseudo-spectral methods. From the 1960s onwards the aerospace industries has been integrated CFD techniques for design, R&D and manufacture of aircraft and jet engines. More recently the methods have been applied to the design of internal combustion engines, combustion chambers of gas turbines and furnaces. Furthermore, routine check-up of drag force, under-bonnet air flow and the in-car environment with CFD by motor vehicle manufacturers. Increasingly CFD become a vital component in the design of industrial products & processes. The main goal is to developments in the CFD field is to provide a strength compare with other CAE (computer-aided engineering) tools such as stress-analysis codes. The main aim why CFD has lagged behind is the tremendous complicity of the underlying behaviour, which preclude a description of fluid flow that is at the same time economical & sufficiently complete. The ability of affordable high-performance computing hardware and the introduction of user-friendly interface have led to a recent up surge of interest, & CFD has entered into the wider industrial community since the 1990s.

There were several unique advantages of CFD over experiment-based approaches to fluid system design:

- Substantial reduce of lead times & costs of new design
- Ability to examine systems where controlled experimentally are difficult or complicate to perform (e.g. very large system)
- Ability to examine systems under hazardous condition at and beyond their normal performance limit (e.g. safety studies and accident scenarios)
- Practically unlimited level of detail of result.

CFD codes were structured around the numerical algorithms that can tackled fluid flow problem. In order to provide easy access to their solving-power all commercial CFD packages include sophisticated user interface to input problem parameter and to examine the result. Hence three main elements contain all codes: (i) a pre-processor, (ii) a solver and (iii) a post-processor. We briefly examined the functions of each of all elements within the content of a CFD code.

3. Modeling & Analysis

In CFD Simulation, there are 3 main steps.

- 1) Pre-Processing
- 2) Solver Execution
- 3) Post-Processing

Pre-Processing is that step where modeling goal is determined and computational grids are created. In second step numeric models and boundary conditions were set to start up solver. Solver excute until the convergence is reached. When solver is terminated, the results are examined which is the post-processing part. The following assumptions are imposed for the computational analysis.

- 1) The flow is steady, completely developed, turbulent and two dimensional.
- 2) The thermal-conductivity of the duct wall, absorber plate & roughness material are independent of temperature.
- 3) The duct wall and absorber plate are homogeneous and isotropic.
- 4) No-slip boundary condition is assigned to the walls in contact with the fluid in the model.
- 5) Negligible radiation heat transfer and other heat losses.

Geometric Modeling (Solution Domain)

The 2-dimensional solution domain used for CFD analysis has been generated in ANSYS version 12.1 (workbench mode) as shown in Fig. 1. The solution domain is a horizontal duct with semicircular rib roughness on the absorber plate at the underside of the top of the duct while other sides are considered as smooth surfaces.

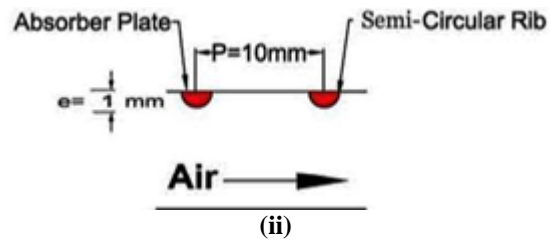
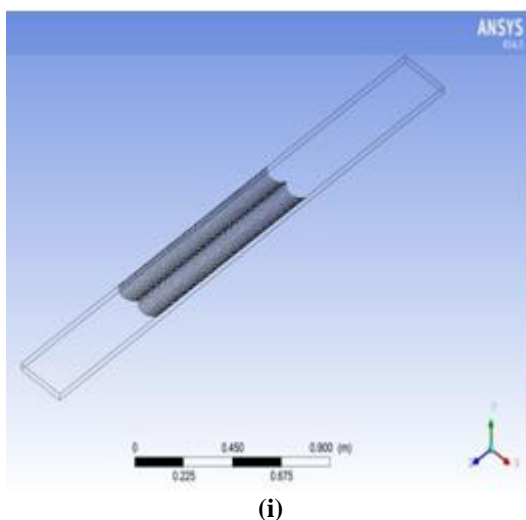


Figure 1: (i) Computational Domain (ii) with semi-circular rib

This duct geometry is partitioned into three sections, namely, entrance, test and exit section respectively. A short entrance length is chosen because for a roughened duct, the thermally fully developed flow is established in a short length 2–3 times of hydraulic diameter. For reducing the end effect of the test section, exit section was used. The top wall consists of a 0.5 mm thick absorber plate made up of aluminum. Artificial roughness created by small diameter galvanized iron (G.I) wire is considered at the underside of the top of the duct on the absorber plate to have roughened surface, running perpendicular to the flowed direction while other side are considering as smooth surfaces. A uniform heat flux of 1000 w/m^2 is considered for computational analysis. The geometrical and operating parameters for artificially roughened solar air heater are listed in Table 1.

Table 1: Range of geometrical and operating parameters for CFD analysis.

Geometrical and operating parameters	Range
Entrance length of duct, ' L_1 '	900 mm
Test length of duct, ' L_2 '	1000 mm
Exit length of duct, ' L_3 '	600 mm
Width of duct, ' W '	200 mm
Depth of duct, ' H '	25 mm
Hydraulic diameter of duct, ' D '	45.45 mm
Rib height, ' e '	2 mm
Rib Pitch, ' P '	10 mm
Reynolds number, ' Re '	2000-16000 (5 values)
Test Angle, ' α '	$15^\circ, 30^\circ, 45^\circ$

Meshing

Meshing of the domain is done using ANSYS ICEM CFD V14.5 software. For semi-circular rib a non-uniform mesh with fine mesh size is used to resolve the laminar sub-layer and is shown in Fig. 2. Since low-Reynolds-number turbulent models are employed, the grids were generated to be very fine. Present non-uniform triangular mesh contained 881616 triangular cells with non-uniform triangular grid of 0.22 mm cell size. This size is suitable to resolve the laminar sub-layer. For grid in-dependency test, the number of cells is varied from 103,231 to 197,977 in 5 steps. It is found that after 161,568 cells, further increase in cells has $< 1\%$ variation in Nusselt number and friction factor values which is taken as criteria for grid independence.

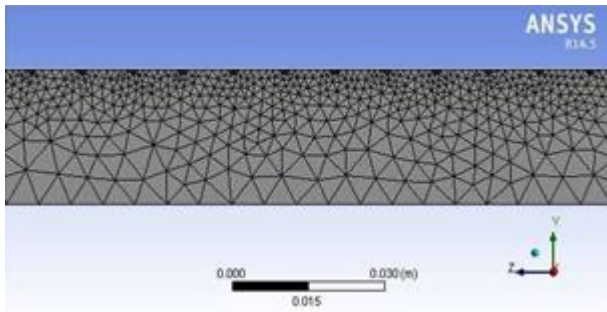


Figure 2

Meshing of computational Domain for semi-circular rib
Boundary conditions

The solution domain of the considered 2d, rectangular duct flow is geometrically quite simple. It is a rectangle on the x–y plane, enclosed by the inlet, outlet and wall boundaries shown in table 2.

Table 2: Boundary conditions used for the present geometry

Edge position	Name	Type
Rear	Inlet	Velocity Inlet
Front	Outlet	Pressure outlet
Top entrance wall	Wall	Wall
Top test wall	Wall	Wall
Top exit wall	Heated Section	Wall
Bottom wall	Wall	Wall

No-slip conditions for velocity in solid surfaces are assumed and the turbulence kinetic energy is set to zero on all solid walls. The top wall boundary condition is selected as constant heat flux of 1000 W/m² and bottom wall is assumed at adiabatic condition. The velocity is introduced uniformly at the inlet while a pres.condition is applied at the outlet exit. The Reynolds number varies from 2000 to 16000 at the inlet. The mean inlet velocity of the flow is calculated using Reynolds number. Constant velocity of air is assumed in the flow direction. The temperature of air inside the duct at the start as 300K. At the exit, a pressure outlet boundary condition is specified with a fixed pressure of 1.013x10⁵ Pa.

The working fluid in all cases is air. The properties of the working fluid (air) and absorber plate material (aluminum) have been assumed to remain constant at average bulk temperature. The thermo-physical properties of working fluid and absorber plate are illustrated in Table 3.

Table 3: Properties of the working fluid (air) and absorber plate

Properties	Working fluid (Air)	Absorber plate (Aluminum)
Density, 'ρ' (kgm ⁻³)	1.225	2719
Specific heat, 'C _p ' (Jkg ⁻¹ K ⁻¹)	1006.43	871
Viscosity, 'μ' (Nm ⁻²)	1.7894e-05	-
Thermal conductivity, 'k'(Wm ⁻¹ K ⁻¹)	0.0242	202.4

Solution method

In the present simulation governing equations of continuity, momentum and energy are solved by the finite volume method in the steady-state regime. The numerical method used in this study is a segregated solution algorithm with a finite volume-based technique. The governing equations are solved using the commercial CFD code, ANSYS FLUENT 14.5. A second-order upwind scheme is chose for energy-

momentum equations. The SIMPLE algorithm (semi-implicit method for press. linked equations) is chosen asscheme to couple pressure-velocity. The convergence criteria of 10⁻³ for the residuals of the continuity equation, 10⁻⁶ for the residuals of the velocity components and 10⁻⁶ for the residuals of the energy are assumed. A uniform air velocity is introduced at the inlet while a pressure outlet condition is applied at the outlet. Adiabatic boundary condition has been implemented over the bottom duct wall while constant heat flux condition is applied to the upper duct wall of test section.

4. Results and Discussion

The effects of relative roughness height and Reynolds number on the heat transfer and friction characteristics for flow of air in a roughened rectangular duct are presented below. The results have been compared with those obtained in case of smooth ducts operating under similar operating conditions to discuss the enhancement in heat transfer and friction factor on account of artificial roughness

3.1 Heat transfer characteristics

The values of Surface temperature drop across the duct generated from CFD for different values of relative roughness height and Reynolds number at a fixed value of roughness pitch as shown below in Figure 3.

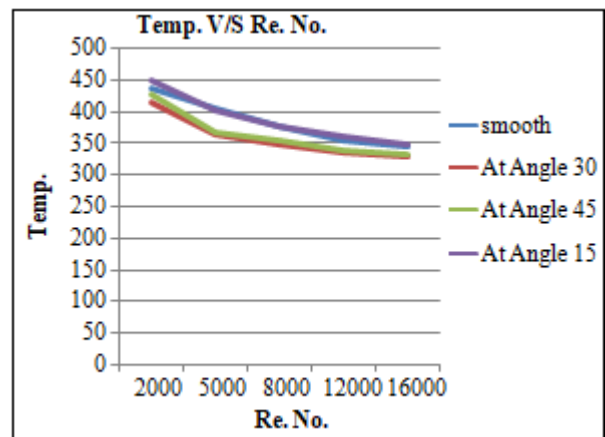
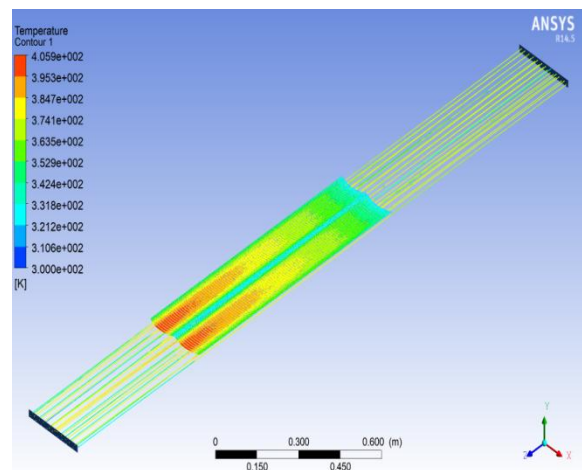
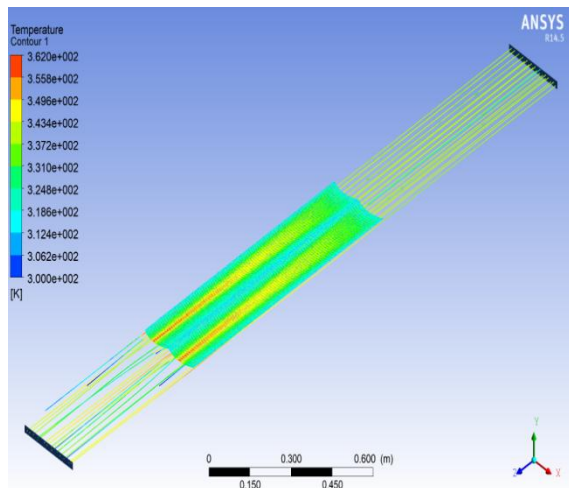


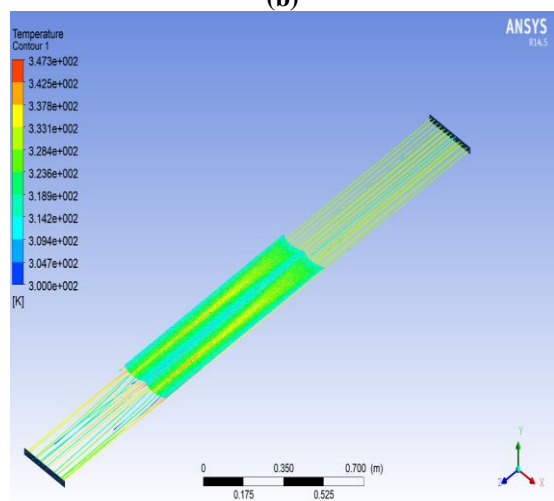
Figure 3



(a)



(b)



(c)

Figure 4: Contour plot of temperature intensity for semi-circular rib (a) Re=5000 (b) Re=12000 (c) Re=16000

The values of heat transfer coefficient generated from CFD for different values of relative roughness height and Reynolds number at a fixed value of roughness pitch with the help of Formulation.

Heat Transfer Coefficient (h)

$$Q = h A \Delta T$$

Average heat transfer coefficient (h) can be obtained directly from FLUENT.

Nusselt Number for roughened duct

$$Nu = h D / K$$

Where k is the thermal conductivity of air and D is the hydraulic diameter.

Nusselt Number for smooth duct

Nusselt Number for smooth roughened duct can be obtained by Dittus–Boelter correlation

$$Nu_s = 0.023 Re^{0.8} Pr^{0.4}$$

Fig. 5. shows the effect of Reynolds number on average Nusselt number for different values of relative roughness height (e/D) and fixed value of roughness pitch (P). The

average Nusselt number is observed to increase with increase of Reynolds number due to the increase in turbulence intensity caused by increase in turbulence kinetic energy and turbulence dissipation rate.

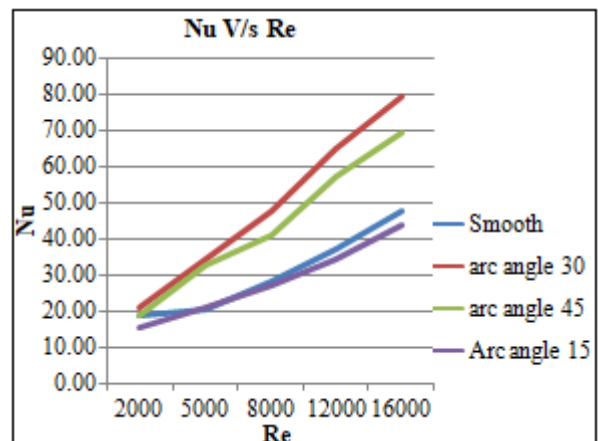
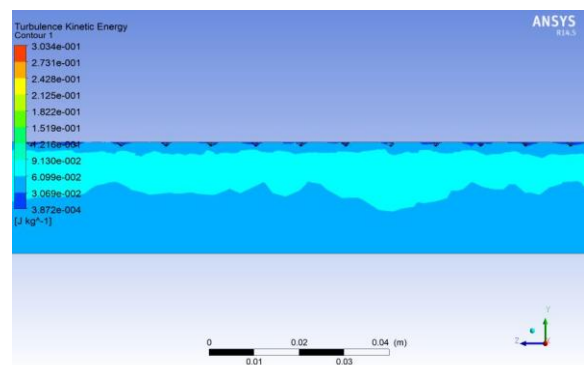


Figure 5: Nusselt number Vs. Reynolds number

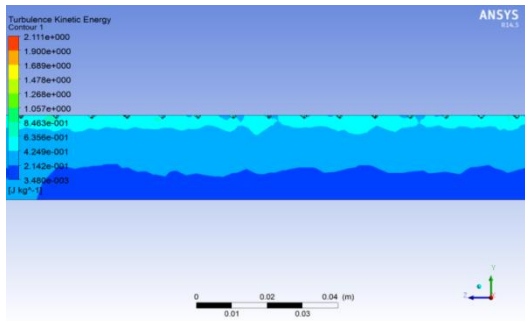
Effect of the relative roughness height (e/d) on heat transfer is also shown typically in Fig. 5. It can be seen that the enhancement in heat transfer of the roughened duct with respect to the smooth duct also increases with an increase in Reynolds number. It can also be seen that Nusselt number values increases with the increase in relative roughness height (e/d) for fixed value of roughness pitch (P). This is due to the fact that heat transfer coefficient is low at the leading edge of the rib and high at the trailing edge. Higher relative roughness height produced more reattachment of free shear layer which creates the strong secondary flow.

The roughened duct having semi-circular rib with relative roughness height of 0.044 provides the highest Nusselt number (Nu_r=79.12) at a Reynolds number of 16000.

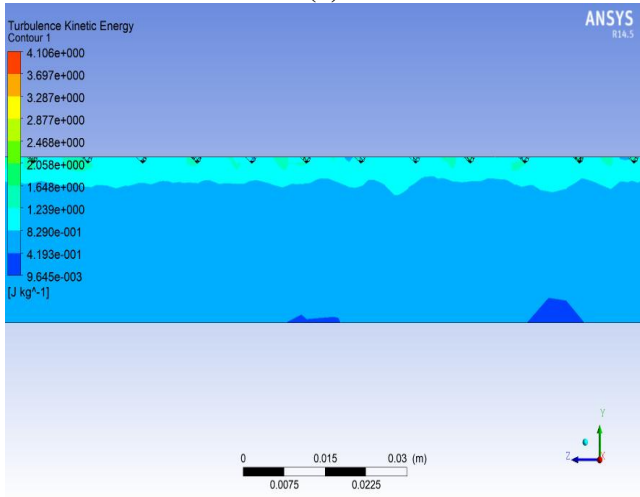
For semi-circular rib the maximum enhancement of average Nusselt number is found to be 1.66 times that of smooth duct for relative roughness height of 0.044 at a Reynolds number of 16000.



(a)



(b)

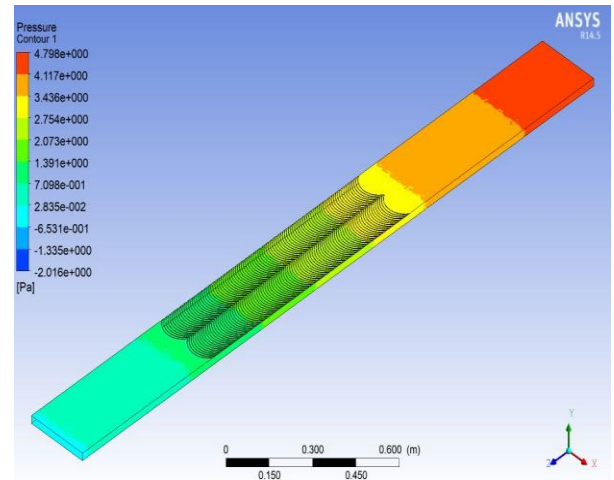
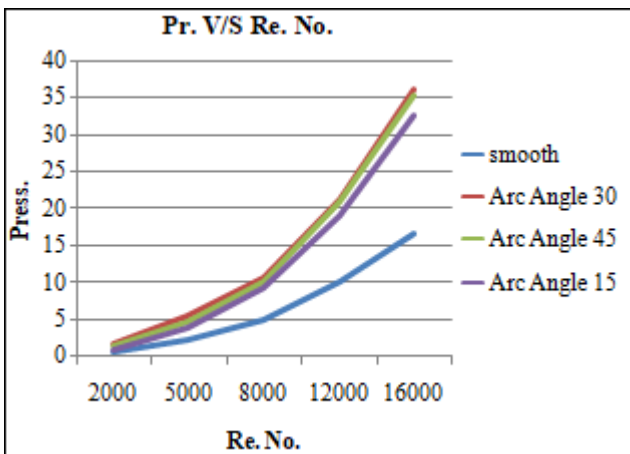


(c)

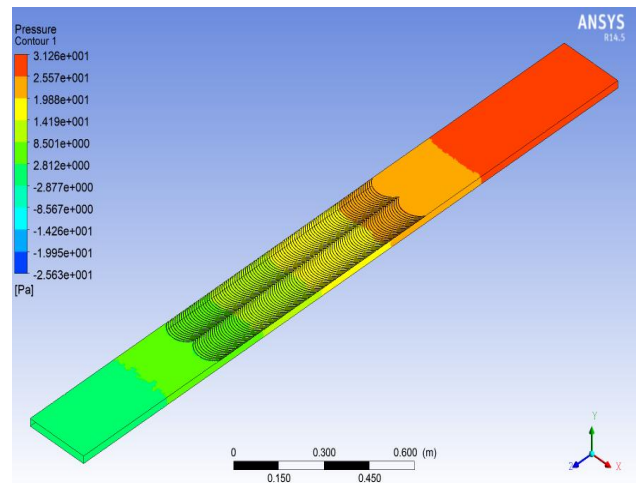
Contour plot of turbulent intensity for semi-circular rib (a) Re=5000 (b) Re=12000 (c) Re=16000

3.2 Fluid friction characteristics

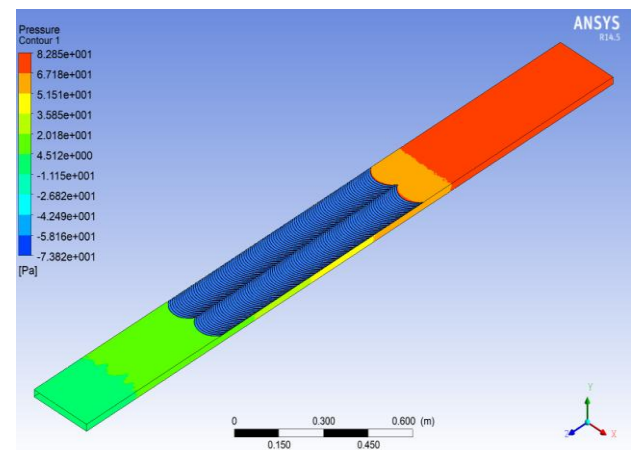
Table 7.3 shows the values of pressure drop across the duct generated from CFD for different values of relative roughness height and Reynolds number at a fixed value of roughness pitch.



(a)



(b)



(c)

Figure 6: Contour plot of pressure for (a) Re=5000 (b) Re=12000 (c) Re=16000

Figure 6 shows the pressure drop across the duct generated from CFD for different values of Reynolds number at a fixed value of roughness pitch.

Fig. 7 shows the effect of Reynolds number on average friction factor for different values of relative roughness height (e/d) and fixed value of roughness pitch. It is observed that the friction factor decreases with increase in

Reynolds number because of the suppression of viscous sub-layer.

Fig 7 also shows that the friction factor decreases with the increasing values of the Reynolds number in all cases as expected because of the suppression of laminar sub-layer for fully developed turbulent flow in the duct. It can also be seen that friction factor values increase with the increase in relative roughness height (e/d) for fixed value of roughness pitch, attributed to more interruptions in the flow path.

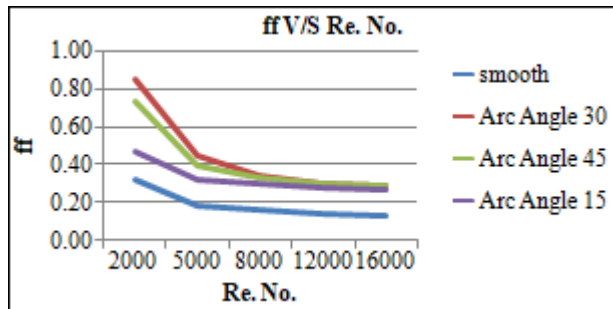


Figure 7: Friction factor Vs. Reynolds number

The roughened duct having semi-circular rib with relative roughness height of 0.044 provides the highest friction factor ($f_f=0.85$) at a Reynolds number of 2000.

For semi-circular rib the maximum enhancement of average friction factor is found to be 2.57 times that of smooth duct for relative roughness height of 0.044 at a Reynolds number of 2000.

The fluid friction phenomenon can be observed and described by the contour of pressure for semi-circular rib. The contour plot of pressure is shown in Fig. 6 (a, b and c). Similar pattern are obtained for contour plot of pressure for semi-circular rib. The flow friction phenomenon can be observed and described by the contour plot of pressure for semi-circular rib.

Thermal enhancement factor

Study of the heat transfer and flow friction characteristics of the artificially roughened ducts shows that an enhancement in heat transfer is accompanied with friction power penalty due to a corresponding increase in the friction factor. The present CFD investigation shows that the roughened duct with relative roughness height (e/d) of 0.044 yields the maximum value of average Nusselt number whereas similar roughened duct with similar relative roughness height (e/d) and roughness pitch results in the maximum value of friction factor. Therefore, it is essential to determine the optimal rib dimension and arrangement that will result in maximum enhancement in heat transfer with minimum friction power penalty. A parameter that facilitates simultaneous consideration of thermal and hydraulic performance as defined by Webb and Eckert is given by Eq. (6.8). A value of this parameter higher than unity ensures the effectiveness of using an enhancement device and can be used to compare the performance of number of arrangements to decide the best among these.

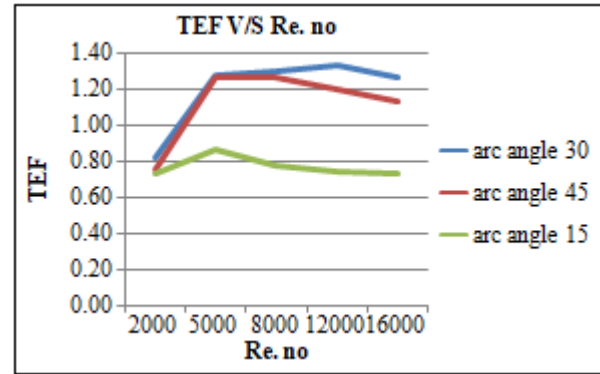


Figure 8: Thermal enhancement factor vs. Reynolds number Fig. 8 shows the variation of the thermal enhancement factor with Reynolds number for all cases. It is found that the thermal enhancement factor values vary between 0.75 and 1.35 for semi-circular rib.

Finally It is observed that roughened duct having semi-circular rib with $e = 2.0$ mm and $P = 10$ mm (i.e. $e/D = 0.044$) gives better thermal enhancement factor ($TEF=1.35$) at a Reynolds number of 12,000.

3.3 Validation of model

In order to validate the present simulated model, the results are compared with available experimental results. Literature search in the area of artificially roughened solar air heater also reveal that the optimum value of relative roughness height generally lies between 0.03-0.047. Table 4.6 shows the comparison of optimum value of relative roughness height between present CFD simulation and available experimental/widely accepted numerical results. On comparison, it has been observed that the optimum value of relative roughness height for present CFD model is found to be 0.044 for semi-circular and circular sectioned rib. The optimum value of relative roughness height from present CFD investigation is found to fall in-between the accepted range i.e. 0.033 and 0.045. It can be seen that there is a good agreement between CFD and experimental/numerical results.

References

- [1] Lanjewar A, Bhagoria JL, Sarviya RM. Heat transfer and friction in solar air heater duct with W-shaped rib roughness on absorber plate. Energy 2011;36:4531-41.
- [2] Mohitkumar G, Gabhane, Amarsingh B, Kanase-Patil, Experimental analysis of double flow solar air heater with multiple C shape roughness Elsevier Solar Energy 155 (2017) 1411-1416
- [3] N.K. Pandey, V.K. Bajpai, Varun, Experimental investigation of heat transfer augmentation using multiple arcs with gap on absorber plate of solar air heater. Solar Energy 134 (2016) 314-326
- [4] Aharwal KR, Gandhi BK, Saini JS. Heat transfer and friction characteristics of solar air heater ducts having integral inclined discrete ribs on absorber plate. Int J Heat and Mass Transfer 2009; 52: 5970-7.
- [5] Hans VS, Saini RP, Saini JS. Heat transfer and friction factor correlations for a solar air heater duct roughened artificially with multiple V-ribs. Sol Energy 2010; 84: 898-91

- [6] Han JC, Zhang YM. High performance heat transfer ducts with parallel broken and V-shaped broken ribs. *International Journal of Heat and Mass Transfer* 1992;35(2):513-23.
- [7] Verma SK, Prasad BN. Investigation for the optimal thermo-hydraulic performance of artificially roughened solar air heaters. *Renewable Energy* 2000; 20: 19–36.
- [8] Singh S, Chander S, Saini JS. Heat transfer and friction factor correlations of solar air heater ducts artificially roughened with discrete V-down ribs. *Energy* 2011; 36: 5053-64.
- [9] Gupta D, Solanki SC, Saini JS. Heat and fluid flow in rectangular solar air heater ducts having transverse rib roughness on absorber plates. *Solar Energy* 1993; 51(1): 31–7.
- [10] Zhang YM, Gu WZ, Han JC. Heat transfer and friction in rectangular channels with ribbed or ribbed-grooved walls. *J. Heat Transfer* 1994; 116 (1): 58–65.
- [11] Park JS, Han JC, Huang Y, Ou S. Heat transfer performance comparisons of five different rectangular channels with parallel angled ribs. *International Journal of Heat and Mass Transfer* 1992;35(11):2891-903..
- [12] Kumar A, Saini RP, Saini JS. Experimental investigation on heat transfer and fluid flow characteristics of air flow in a rectangular duct with Multi v-shaped rib with gap roughness on the heated plate. *Solar Energy* 2012; 86:1733–49.
- [13] Chaudhary S, Varun, Chauhan MK. Heat transfer and friction factor characteristics using continuous M shape ribs turbulators at different orientation on absorber plate solar air heater. *Int J energy and environment* 2012; 3(1):33-48.
- [14] Sharma AK, Thakur NS. CFD based fluid flow and heat transfer analysis of a v- shaped roughened surface solar air heater. *Int J Engineering Science and Technology* 2012;4 (5):2115-21.
- [15] Yadav AS, Bhagoria JL. A CFD analysis of a solar air heater having triangular rib roughness on the absorber plate. *International Journal of ChemTech Research* 2013; 5(2): 964-71.
- [16] Amraoui MA, Aliane K. Numerical Analysis of a Three Dimensional Fluid Flow in a Flat Plate Solar Collector. *International Journal of Renewable and Sustainable Energy* 2014; 3(3): 68-7
- [17] Wang HT, Lee WB, Chan J, To S. Numerical and experimental analysis of heat transfer in turbulent flow channels with two-dimensional ribs. *Applied Thermal Engineering* 2015; 75: 623-634.
- [18] Prasad BN, Kumar A, Singh KDP. Optimization of thermo hydraulic performance in threesidesartificially roughened solar air heaters. *Solar Energy* 2015;111: 313–319.
- [19] Singh S, Singh B, Hans VS, Gill RS. CFD (computational fluid dynamics) investigation on Nusselt number and friction factor of solar air heater duct roughened with non-uniformcross-section transverse rib *Energy xxx* (2015) 1-9
- [20] Singh S, Chander S, Saini JS. Thermo-hydraulic performance due to relative roughness pitch in V-down rib with gap in solar air heater duct—Comparison with similar rib roughness geometries. *RenewableandSustainableEnergyReviews* 2015;43: 1159–1166.
- [21] Yadav AS, Bhagoria JL. Heat transfer and fluid flow analysis of solar air heater: a review of CFD approach. *Renewable and Sustainable Energy Reviews* 2013; 23: 60-79.
- [22] Launder BE and Spalding DB. *Lectures in mathematical models of turbulence*. London, England: Academic Press; 1972
- [23] Chaube A, Sahoo PK, Solanki SC. Analysis of heat transfer augmentation and flow characteristics due to rib roughness over absorber plate of a solar air heater. *Renewable Energy* 2006; 31: 317-31.
- [24] Ryu DN, Choi DH, Patel VC. Analysis of turbulent flow in channels roughened by two-dimensional ribs and three-dimensional blocks. Part I: Resistance. *International Journal of Heat and Fluid Flow* 2007; 28: 1098–1111.
- [25] Layek A, Saini JS, Solanki SC. Heat transfer and friction characteristics for artificially roughened ducts with compound turbulators. *InternationalJournal of Heat and Mass Transfer* 2007; 50: 4845–54.
- [26] Kamali R, Binesh AR. The importance of rib shape effects on the local heat transfer and flow friction characteristics of square ducts with ribbed internal Surfaces. *International Communications in Heat and Mass Transfer* 2008; 35: 1032–1040.
- [27] Saini RP, Verma J. Heat transfer and friction factor correlations for a duct having dimple-shaped artificial roughness for solar air heaters. *Energy* 2008; 33: 1277–87.
- [28] Saini SK, Saini RP. Development of correlations for Nusselt number and friction factor for solar air heater with roughened duct having arc-shaped wire as artificial roughness. *Solar Energy* 2008; 82: 1118–30.
- [29] Aharwal KR, Gandhi BK, Saini JS. Heat transfer and friction characteristics of solar air heater ducts having integral inclined discrete ribs on absorber plate. *Int J Heat and Mass Transfer* 2009; 52: 5970–7.
- [30] Bopche SB, Tandale MS. Experimental investigations on heat transfer and frictional characteristics of a turbulator roughened solar air heater duct. *Int J Heat and Mass Transfer* 2009; 52: 2834–48.
- [31] Lanjewar A, Bhagoria JL, Sarviya RM. Heat transfer and friction in solar air heater duct with W-shaped rib roughness on absorber plate. *Energy* 2011;36:4531-41.
- [32] Hans VS, Saini RP, Saini JS. Heat transfer and friction factor correlations for a solar air heater duct roughened artificially with multiple V-ribs. *Sol Energy* 2010; 84: 898–91
- [33] Singh S, Chander S, Saini JS. Heat transfer and friction factor correlations of solar air heater ducts artificially roughened with discrete V-down ribs. *Energy* 2011; 36: 5053-64.
- [34] Kumar A, Saini RP, Saini JS. Experimental investigation on heat transfer and fluid flow characteristics of air flow in a rectangular duct with Multi v-shaped rib with gap roughness on the heated plate. *Solar Energy* 2012; 86:1733–49.
- [35] Chaudhary S, Varun, Chauhan MK. Heat transfer and friction factor characteristics using continuous M shape ribs turbulators at different orientation on absorber plate solar air heater. *Int J energy and environment* 2012; 3(1):33-48.

- [36] Sharma AK, Thakur NS. CFD based fluid flow and heat transfer analysis of a v- shaped roughened surface solar air heater. Int J Engineering Science and Technology 2012;4 (5):2115-21.
- [37] Yadav AS, Bhagoria JL. A CFD analysis of a solar air heater having triangular rib roughness on the absorber plate. International Journal of ChemTech Research 2013; 5(2): 964-71.
- [38] Amraoui MA, Aliane K. Numerical Analysis of a Three Dimensional Fluid Flow in a Flat Plate Solar Collector. International Journal of Renewable and Sustainable Energy 2014; 3(3): 68-75.